Int. J. Heat Mass Transfer. Vol. 10, pp. 529–539. Pergamon Press Ltd. 1967. Printed in Great Britain

THE EFFECT OF FLUID TURBULENCE ON THE RATE OF HEAT TRANSFER FROM SPHERES

WILLIAM J. LAVENDER* and DAVID C. T. PEI†

(*Received* 25 *July* 1966 *and in revised form* 27 *September* 1966)

Abstract—The rate of heat transfer from a 1·25-in dia. sphere was studied in a vertical wind tunnel. Results in both heat transfer and drag indicate that the product of Reynolds number and turbulence intensity, which is defined as the turbulent Reynolds number, is an important parameter, and that the scale of turbulence is of minor significance.

NOMENCLATURE

A_0,	fraction of open area of a turbulence generating grid (dimensionless);
a,	constant, [ft^{-1}];
b,	constant, [dimensionless];
C_D,	drag coefficient [dimensionless];
D,	body diameter [ft];
g_c,	gravitational constant [ft/s^2];
k,	thermal conductivity [Btu/h ft°F];
L_x, L_y,	scale of turbulence [ft];
M,	mesh size of a grid [ft];
Nu,	Nusselt number [dimensionless];
Δp_1, Δp_0,	pressure differential at distance y in free stream [lb/in^2];
Pr,	Prandtl number [dimensionless];
Re,	Reynolds number [dimensionless];
Re_T,	turbulent Reynolds number as defined by equation (4) [dimensionless];
R_y,	normalized correlation coefficient [dimensionless];
r,	range of integration [ft];
T,	turbulence intensity for unidirectional flow [dimensionless];
$\%T$,	percentage of turbulence [dimensionless];
U',	mean bulk velocity of the fluid [ft/s];
U_0,	free stream velocity [ft/s];
U_1,	free stream velocity in body wake [ft/s];
u,	fluctuating component of velocity [ft/s];
X,	distance downstream from the turbulence generating grid [ft];
y,	displacement from centre line of flow [ft];
α,	constant [dimensionless];
ρ,	density [lb/ft^3];
ν,	kinematic viscosity [ft^2/h].

INTRODUCTION

INVESTIGATION of convective heat transfer have been very successful, both from an experimental and theoretical point of view. However, thus far, work in turbulent flow has been restricted largely to the structure of turbulence [1–4]. Therefore, it becomes necessary in most engineering problems to precede the theoretical analysis with extensive experimental investigations. The purpose is two fold; (i) to provide a usable correlation, and (ii) to provide data for the substantiation of theoretical models.

In 1948, Comings, Clapp and Taylor [5] published one of the first studies on the rate of heat and mass transfer from cylinders in a

* W. J. Lavender, Delmar Chemicals Limited, Montreal, P.Q.

† D. C. T. Pei, Chemical Engineering, University of Waterloo, Waterloo, Ontario.

turbulent air stream. The portion of their work which is most frequently quoted by others in the field is the plot showing the effect of turbulence level on Nusselt number at a constant Reynolds number. However, on plotting Nusselt number against Reynolds number, a series of lines corresponding to different ranges of turbulence levels are needed to represent their data.

Experimental data on spheres was first reported in 1957 by Hsu and Sage [6]. However, no attempt was made to study the overall effects of turbulence in the main flow. At about the same time, Van der Hegge Zijnen [7], produced a most comprehensive study for the case of cylinders, in which both turbulence intensity and the scale of turbulence were considered. His data were then correlated by means of the following equation

$$Nu/Nu_0 = 1 + \Phi\left(\frac{u'D}{\nu}\right)\Psi\left(\frac{L_x}{D}\right) \quad (1)$$

where Nu/Nu_0 represents the fractional increase in the Nusselt number due to turbulence. He also reported that a maximum increase in the heat-transfer rate occurred at the same value of the group L_x/D regardless of turbulence level. Again, the data were represented by a series of curves, and these correlations obtained "are the result of successive approximations and smoothing out of sometimes non-systematic scatter."*

In contrast to other workers, Yuge [8], claimed that turbulence in the main flow has no marked effect on the heat-transfer rate from an internally heated sphere at higher Reynolds numbers. However, a close examination of the series of correlations which he proposes will reveal that his data are about 30 per cent higher than the rates predicted by the generally accepted Froessling equation [9]. Another interesting point to note in Yuge's report is that he found increases in the Nusselt number well above 50 per cent when a small hoop was attached to the forward surface of the sphere. Unfortunately, he did not include his measurements for these experiments.

In 1964, Sage [10], again proposed a method of predicting thermal and material transport from spheres, this time relating directly the rate of transport to turbulence intensity. Two shortcomings are apparent: (i) only the graphical correlations of the experimental data for a single sphere are presented, and (ii) the levels of turbulence were not measured by the experimenters, but rather, it was assumed that the turbulence characteristics were identical to those found by Davis [3, 4].

The above works all represent a considerable amount of effort, but unfortunately, no single correlation seems quite compatible with the data of any other worker. Therefore, it has been the intention of this author to examine systematically the various turbulence parameters affecting the thermal transport from a sphere and attempt to seek a single correlation.

PRINCIPAL CONSIDERATIONS

Numerical solutions of the Navier–Stokes equations for heat transfer have long since shown that in laminar flow systems, the Nusselt number exhibits a Reynolds number power dependency of 0·5 [9]. Similarly, a solution of the problem of heat transfer from a sphere to an infinite stagnant medium shows that the Nusselt number is constant at 2·0 [9]. Hence, the relation between Nusselt and Reynolds numbers is generally accepted as:

$$Nu = 2 + \alpha Re^{0\cdot 5} \quad (2)$$

where "α" is a function of the Prandtl number of the fluid. The widely quoted correlation for spheres is that of Froessling (9):

$$Nu = 2\cdot 0 + 0\cdot 6\, Re^{0\cdot 5}\, Pr^{0\cdot 33}. \quad (3)$$

Therefore, in any turbulent heat-transfer correlation, it is desirable to retain the Reynolds power of 0·5.

The influence of turbulence is generally conceded as causing an increase in the rate of heat transfer from spheres due to the penetration

* Quoted from reference [7].

of the boundary layer by energy-dissipating fluid eddies. Hence, for the case of a sphere, a coupling of two mechanisms is involved in the process: (i) the natural boundary layer turbulence produced by flow around a body, and, (ii) the pseudo-boundary layer turbulence produced by eddies from the free stream penetrating the boundary layer.

From studies of the effect of free stream turbulence on the drag coefficient, [11, 12] it has been well established that when a particle is immersed in an increasingly turbulent flowing fluid, the Reynolds number at transition decreases as the turbulence level in the stream increases. That is, as the turbulence level increases, the critical Reynolds number decreases, although not all reports are agreeable as to the rate of this decrease. Thus, it is normal to anticipate that free stream turbulence would promote transition at a lower Reynolds number than encountered when the main stream is free of turbulence. Simultaneously, then, the characteristic sharp decrease in drag coefficient which occurs at transition should be evident when the combination of the above two mechanisms is large enough to produce an earlier transition. This sharp drop should also then be accompanied by a marked increase in heat-transfer rate as found with laminar free streams if this coupling mechanism is valid.

If the process is visualized as the penetration of the boundary layer by fluid eddies from the free stream, then obviously the number of eddies or turbulence intensity would be expected to exert the most influence on the rate of heat transfer. Secondly, the size of the eddies would exert some influence since the amount of boundary layer disruption and energy dissipation will be proportional to the eddy size; that is, some function of the scale of turbulence.

In particular, since turbulence intensity is itself a velocity measurement, it is natural to anticipate some sort of interaction between intensity and Reynolds number. That is, turbulence intensity would be expected to have some modifying effect on the Reynolds number, either in an additive or multiplicative fashion. Thus, one can define such terms as:

$$Re_T = \frac{\sqrt{\overline{u^2}}}{U} \times \frac{UD}{\nu} = \frac{\sqrt{(\overline{u^2}D^2)}}{\nu} = T \times Re \quad (4)$$

and

$$Re' = \frac{(U + \sqrt{\overline{u^2}})\,D}{\nu} = \frac{UD}{\nu} + \frac{\sqrt{(\overline{u^2}D^2)}}{\nu} = Re + Re_T. \quad (5)$$

Thus, both combinations contain a Reynolds number calculated from the fluctuating velocity component. This is defined as the turbulent Reynolds number. In addition, to include the scale of turbulence in a dimensionless form, the ratio of scale of turbulence to sphere diameter is defined as L_y/D. Finally, it would be reasonable to expect that the turbulent heat-transfer rate can be expressed by some function of the above parameters, i.e.:

$$Nu = f(Re, Re_T, L_y/D) \quad (6)$$

wherein it is understood that T and L_y may not be state variables, but may be dependent on the geometry of the turbulence generating grid, that is, on the variables X/M and A_0 and hence,

$$Nu = f(Re, T, L_y/D, A_0, X/M). \quad (7)$$

EXPERIMENTAL

Frequently, when experimental data obtained from the literature are analysed, anomalies exist for which there is no obvious reason. It must be assumed that basic differences in experimental equipment and techniques are the cause. Keeping this in mind, detailed information on experimental conditions, such as the following, is included.

Apparatus

To provide a sturdy, compact and highly flexible system for the investigation of the effects of wide ranges of the turbulence parameters, a vertical wind-tunnel was designed and constructed. Basically, it consists of a high-speed turbo-compressor whose outlet discharged vertically upwards through a copper pipe and through a 6°-tapered wooden cone which enabled divergence of the flow into a transparent acrylic test section of larger diameter than the copper pipe. A long calming section was provided to ensure fully developed flow in the test section. The discharge section of the tunnel assembly was another piece of acrylic tubing of the same diameter as the test section.

The turbulence grids were perforated plates with holes on equilateral spacings and screens of the conventional woven square-mesh type. Table 1 gives the description of the turbulence generators.

Figure 1 shows a top and side view of the test section and the accompanying instrumentation. Two hot-wire probes were mounted on opposite sides of the tunnel with slide assemblies to enable accurate positioning of the probes. One probe was adjustable only on the diameter of the section by a micrometer drive, while the other could be positioned in a vertical plane on the diameter of the tunnel.

The test piece, a 1·25-in dia. sphere, was inserted through a hole and mounting mechanism in the tunnel wall at a 45° angle to the micrometer-adjustable probe, but in the same plane. A locking set-screw permitted accurate positioning and withdrawal of the sphere to the wall of the tunnel while free stream properties were measured. On the same axis as, but remote from the sphere, an 0·125-in dia. compact pitot tube was inserted $3\frac{1}{2}$ in above the plane of the probes to enable mean velocity measurements in the wake of the sphere as well as in the free stream.

After several attempts to design a sphere which can be readily manufactured and uniformly heated, the sphere shown in Fig. 2 was found to be adequate. It consists of a hollow ball machined as two hemispheres, having a $\frac{1}{8}$-in wall thickness and a drilled stem attached for mounting and introduction of a heating wire.

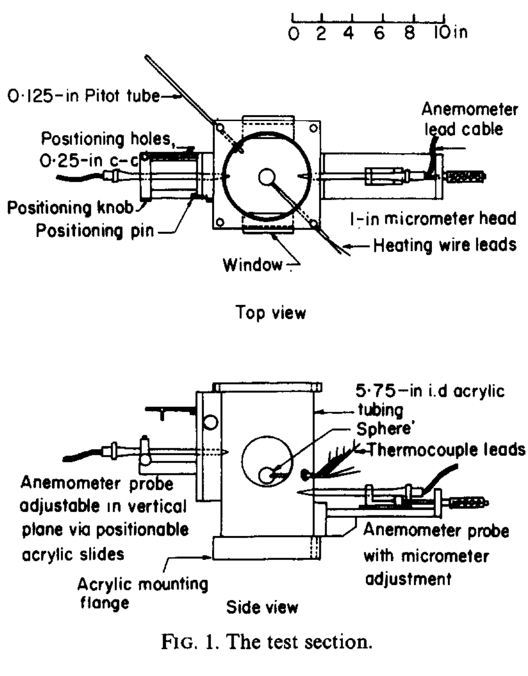

FIG. 1. The test section.

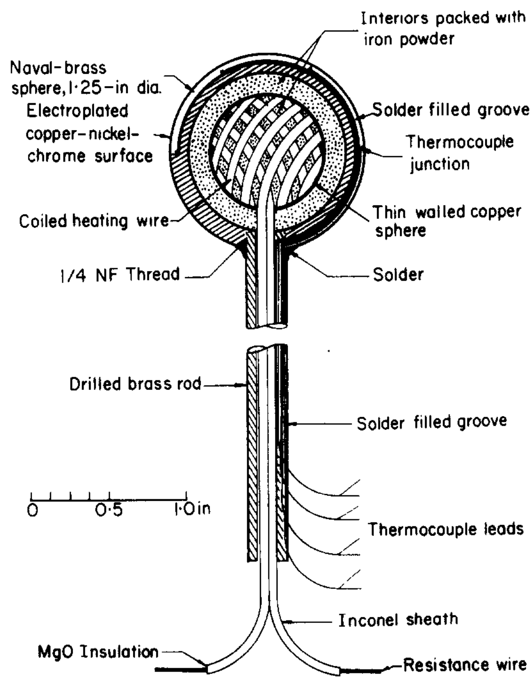

FIG. 2. Cross section of the test sphere.

Naval brass was used because of its relatively large thermal conductivity, strength and high melting point.

To eliminate hot spots on the surface of the sphere, it was desirable to keep the heating wire from directly contacting the internal surface of the sphere. This was accomplished by coiling $3\frac{1}{2}$ ft of electrically insulated Thermocoax heating wire inside a thin copper sphere and mounting it centrally inside the brass sphere. Moreover, to provide uniformity of heat flux, the interiors of both spheres were packed tightly with finely ground iron powder. The powder had a thermal conductivity of about half that of the brass and thus permitted a faster approach to equilibrium and a smaller temperature difference between the brass and heating wire than was possible with the graphite packings tried initially.

The entire surface of the sphere was then highly polished and electroplated with succeeding layers of copper, nickel and chrome to provide an untarnishable, hard, low-radiating surface. The thermocouples were then calibrated by immersing the entire sphere in various liquids at their known boiling points.

Power was supplied to the heating wire by a variable 360 W electronic current stabilizer, and was monitored by a combination of accurate resistors which provided stepped-down voltages that could be read on a Leeds–Northrup 0·001-mV sensitivity potentiometer.

Procedure

With the turbocompressor running, a turbulence generator in position, and the sphere positioned in the centre of the test section, an amount of current was introduced such that a temperature difference between sphere and air stream of about 180 degF was obtained. Equilibrium was determined as being established when the sphere thermocouples indicated constant temperatures for a period of not less than $\frac{1}{2}$ h.

At that time, the sphere and free stream thermocouple readings were recorded, as well as the current input and voltage drop across the heating wire. The power to the sphere was then switched off and the sphere withdrawn to the wall of the tunnel to enable a velocity profile determination with the pitot tube and a single level of turbulence measurement with a hot-wire anemometer probe at the centre of the tunnel.

The scale of turbulence was next determined by reading from a Random-Signal Correlator the correlation coefficient provided by the simultaneous signals from the two hot-wire probes. Readings were taken at 0·020-in intervals over a distance of 0·100 in starting with an 0·020-in probe separation, and at 0·100-in intervals over the next 0·900 in. The correlation coefficient at zero separation was assumed to be 1·0 in accordance with standard practice. Typical curves are shown in Fig. 3.

This overall procedure was then repeated for a series of velocities ranging from 10 ft/s to 130 ft/s for each of the turbulence generators listed in Table 1, as well as for the free stream without a turbulence grid.

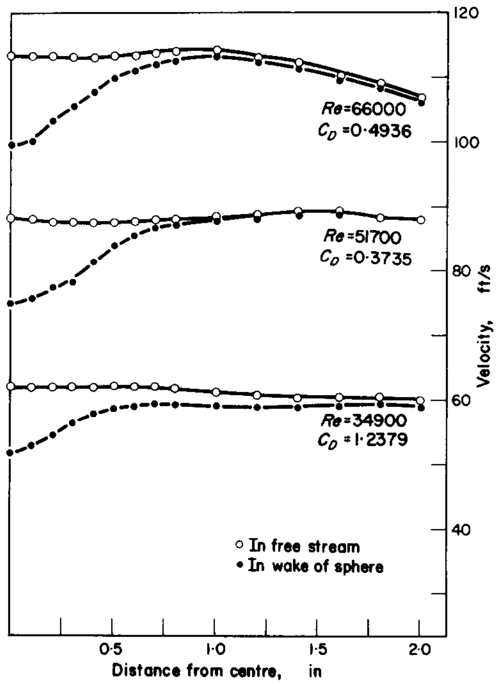

FIG. 3. Typical velocity profiles.

Table 1. Turbulence generating grids

Woven square mesh screens			
Mesh	Wire dia. (in)	Open area (%)	Material
4	0·041	69·9	s. steel
6	0·028	69·6	s. steel
12	0·023	51·8	s. steel
20	0·010	64·0	s. steel
30	0·0085	55·4	s. steel
50	0·0075	39·1	brass

Perforated plates				
Hole dia. (in)	Hole centres (in)	Thickness (in)	Open area (%)	Material
0·1875	0·2500	0·035	50·7	steel
0·375	0·4375	0·035	70·0	steel
0·625	0·6875	0·035	99·0	steel
9·250	0·5000	0·250	28·6	acrylic
0·500	0·7500	0·250	38·6	acrylic

In accordance with the standard procedure in estimating the drag coefficient, velocity measurements across the radius of the tunnel were made with the pitot tube, both in the free stream and in the wake of the sphere. Pressure differential readings were made using a Betz manometer with a sensitivity of $\pm 0{\cdot}05$ mm of water. Measurements were taken at 0·1-in intervals over the first 0·8 in and at 0·2-in intervals over the next 1·2 in.

Calculations

Nusselt and Reynolds numbers were calculated using the arithmetic average of the average sphere temperature and the free stream temperature. Since only two-thirds of the heating wire was actually contained within the sphere, that fraction of the total power input was used in determining the Nusselt number. In addition, correction for the small radiant heat loss was also taken into account.

The turbulence intensity was directly calculable from the anemometer readings, whereas the scale of turbulence required integration of the correlation coefficient vs. separation distance curve. The latter was obtained by first piece-wise fitting two exponential equations of the form:

$$R_y = \exp(-ay) \tag{8}$$

and

$$R_y = b \exp(-ay) \tag{9}$$

to the curves using a "least-squares" method. The scale was then determined by the integration of the combination of these functions from $y = 0$ to $y = \infty$, as required by the definition of the scale of turbulence.

Using curves such as those shown in Fig. 3, the drag coefficient was calculated. To avoid influence of the tunnel-wall boundary layer, the range of integration was the same as that of the measurements, i.e. 2·0-in radius. It will be noted that the calculations also involved the assumption that the velocity profile was cylindrically symmetrical about the centre of the tunnel and hence this assumption plus the range of integration make the drag coefficients only semi-quantitative in nature.

RESULTS

A preliminary analysis of the above results was conducted by plotting the data as Nusselt number against Reynolds number and comparing it to some of the correlations and data available from other workers in the forced convective heat-transfer field. The graph is shown in Fig. 4. Clearly, the author's data lies much closer to the extended correlations of Williams [19] and McAdams [20], than to the Ranz-Marshall laminar flow correlation [20], whereas Yuge's data [8], lies closer to the laminar correlation. The data of Sage [10] and Comings, Clapp and Taylor [5] on the other hand, appear to be scattered with respect to any of these correlations. Hence, it is obvious that Nusselt and Reynolds numbers alone are definitely not sufficient parameters to represent the turbulent heat-transfer picture.

To remain completely objective in the treatment of data, experimental values of the flow

Table 2. Perforated plate data

Reynolds number (1)	Nusselt number (2)	Turbulence level (%) (3)	Scale of turbulence (ft) (4)	Hole dia. (in) (5)
10571	80·24	4·65	0·1003	0·1875
37255	171·73	3·15	0·0211	0·1875
49972	212·45	2·96	0·0134	0·1875
10866	99·20	11·18	0·0189	0·25
32630	198·10	9·64	0·0091	0·25
46913	255·67	9·41	0·0052	0·25
17970	109·60	5·03	0·0416	0·375
27616	144·49	4·44	0·0232	0·375
33020	164·13	4·23	0·0169	0·375
50813	306·81	13·05	0·0073	0·500
32302	216·83	14·06	0·0078	0·500
18465	156·59	16·79	0·0093	0·500
56924	248·23	4·62	0·0125	0·625
37858	188·45	5·02	0·0155	0·625
13600	92·64	6·68	0·0446	0·625
4986	54·14	13·30	0·0773	0·625
9429	74·94	7·94	0·0917	0·625
15251	100·42	6·74	0·0732	0·625
20833	122·42	6·39	0·0500	0·625
28417	152·48	5·76	0·0372	0·625
38354	190·80	5·37	0·0261	0·625
45796	222·30	4·96	0·0187	0·625
54250	245·04	4·64	0·0167	0·625
60036*	273·03	5·15	—	0·625
7231†	78·31	9·84	—	0·625

* ΔT = 10°F.
† ΔT = 20°F.
Tables 2–5 give the calculated experimental data recorded in this work.

parameters were then subjected to regression analysis for the purpose of determining the important parameters and their relation to the Nusselt number. Piecewise analysis of the data and the calculation of a statistical multiple correlation coefficient enabled this to be done using the computerized regression analysis program.* The ranges of parameters included in this analysis are as follows:

(1) Reynolds number 2000–65000
(2) Nusselt number 35–300
(3) Turbulence level (%) 1–17
(4) Scale of turbulence (ft) 0·007–2·0
(5) Opening of grids (in) $\frac{3}{16}$–$\frac{5}{8}$ in dia. and 4–50 in mesh size.

* Copies of the calculated experimental data and the computer program are available on request.

The results clearly indicated that if L_y and T are measured downstream from the grid, the grid geometry and position are not required to characterize the flow, and that L_y is of minor significance as compared to turbulence level. Therefore, analysis of the data was reduced to the seeking of a correlation in terms of the equations (4) and (5); that is, using a turbulent Reynolds number. To this end the ratio of $(Nu - 2)/Re^{0.5}$ was plotted against the turbulent Reynolds number, in an effort to obtain an equation which would yield at low turbulence

Table 3. Woven screen data

Reynolds number (1)	Nusselt number (2)	Turbulence level (%) (3)	Scale of turbulence (ft) (4)	Mesh size (5)
50787	200·86	2·21	—	4
15091	96·76	4·21	—	4
50313	206·71	2·62	—	4
12046*	97·19	5·09	—	4
55372*	233·09	2·68	—	4
62535	231·50	2·42	0·0551	6
11876	81·56	3·82	0·1667	12
39963	166·81	2·30	0·0613	12
54730	207·98	1·98	0·0501	12
55966	210·13	1·11	0·1246	30
38170	163·18	1·37	0·2568	30
12362	86·60	3·06	0·8438	30
1935	36·21	10·91	0·9677	30
6156	60·16	4·08	0·6658	30
7880	66·94	3·44	0·7680	30
9604	74·68	3·24	0·7645	30
11839	84·07	3·00	1·8442	30
14806	96·39	2·79	1·6144	30
18521	108·35	2·36	1·2677	30
26255	131·00	1·79	0·6053	30
31987	144·83	1·40	0·4539	30
38331	160·46	1·20	0·1282	30
49433	188·62	0·98	0·0918	30
46827	186·44	1·87	0·0106	50
42125	173·81	2·09	0·0112	50
43124	174·05	0·88	0·0221	50
34937	152·79	0·99	0·0325	50
32937	145·40	1·06	0·0484	50
26061	127·34	1·38	0·0824	50
20592	113·08	1·74	0·1184	50
17551	102·71	2·06	0·1391	50
12414	85·87	2·76	0·1831	50
7574	65·60	3·55	0·2224	50
4222	50·43	6·27	0·3876	50

* Hoop attached; 0·052-in dia. copper wire.

Table 4. No turbulence generator

Reynolds number	Nusselt number	Turbulence level (%)	Scale of turbulence (ft)
49550	192·07	4·15	0·0520
43470	177·67	4·26	0·0533
32378	146·75	4·14	0·0554
26405	127·62	4·38	0·0609
19486	109·41	5·24	0·0623
17377	101·59	5·64	0·0641
14496	91·83	6·34	0·0711
9402	71·65	7·74	0·0679
4900	53·10	13·66	0·0481

Table 5. Profile drag data

Reynolds number	Drag coefficient	Turbulence level (%)	Turbulence generator
66000	0·4936	4·99	0·625 grid
65300	0·3691	2·34	10 mesh
62400	1·0620	1·74	20 mesh
60200	0·9521	0·96	30 mesh
50000	1·2066	1·06	30 mesh
38900	1·1479	1·82	20 mesh
56100	1·1314	1·95	10 mesh
51700	0·3735	2·30	0·375 grid
52200	0·5261	2·78	0·625 grid
46250	0·5780	2·89	0·625 grid
45100	0·7154	1·32	0·375 grid
46500	1·1353	1·60	10 mesh
45100	1·2167	1·18	20 mesh
43400	1·1835	1·10	30 mesh
33500	1·1142	1·38	30 mesh
34910	1·2379	1·30	20 mesh
36020	1·1661	1·55	10 mesh
34690	1·0265	2·09	0·375 grid
35960	1·2354	2·62	0·625 grid
63040	0·4173	2·33	0·375 grid
65360	1·1336	1·43	10 mesh

levels, the laminar flow heat-transfer equation. The factor of $Pr^{0\cdot 33}$ has been omitted since the Prandtl number was essentially constant at 0·674 in this investigation. Thus, the resulting equation would have the form:

$$Nu = 2 + f(Re_T)\, Re^{0\cdot 5} \qquad (10)$$

where $f(Re_T)$ is the function of turbulent Reynolds number obtained graphically.

Figure 5 illustrates the results of this reasoning; the relation is essentially linear with a sharp increase in heat-transfer rates occurring at about $Re_T = 1000$. A "least-squares" method of curve fitting yielded the following relations

$$Nu = 2 + 0\cdot 629\, Re^{0\cdot 5}\, Re_T^{0\cdot 035} \qquad (Re_T < 1000) \qquad (11)$$

$$Nu = 2 + 0\cdot 145\, Re^{0\cdot 5}\, Re_T^{0\cdot 250} \qquad (Re_T > 1000) \qquad (12)$$

with a maximum deviation of ± 10 per cent.

Similarly, when the data of Yuge [8] are plotted, the heretofore multiple lines are reduced to a single correlation:

$$Nu = 2 + 0\cdot 339\, Re^{0\cdot 5}\, Re_T^{0\cdot 085} \qquad (13)$$

although the curve is much below that of the author.

Finally, an investigation was launched to determine the cause of the sharp increase in heat-transfer rates at about $Re_T = 1000$. As boundary layer turbulence enhanced by the free stream turbulence, a drop in the drag coefficient should also be in evidence. Figure 6 was prepared to show that this is indeed the case. Even though the drag coefficient values are only semi-quantitative, this figure indicates over a range of Reynolds number a steep decline in profile drag and that this also occurs at about $Re_T = 1000$.

DISCUSSION

Figure 5 indicates the results of the regression analysis for Nusselt number dependency on the previously mentioned turbulence parameters. Although L_v/D exhibited some significance, it was found that the modification of Reynolds number by turbulence intensity alone was sufficient to adequately correlate the data, and that T and L_v are indeed state variables, independent of X/M and A_0. The simplicity of this correlation is obvious; it produces an equation of the form of Froessling's streamline heat-transfer equation, and in the limit of $Re_T = 6\cdot 5 \times 10^{-3}$ the equations are identical. That is, for a turbulent

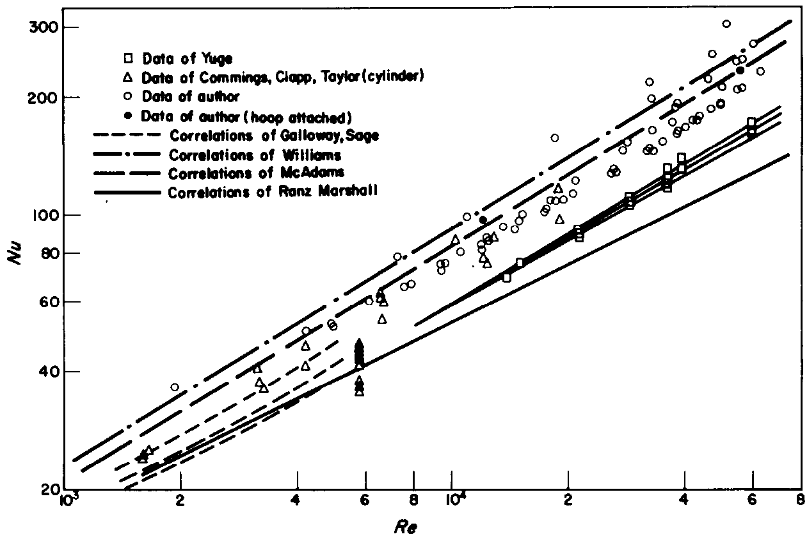

FIG. 4. Relation between Nusselt and Reynolds numbers.

Reynolds number larger than this value, the Froessling equation no longer applies.

Another significant point in Fig. 5 to note is the sharp increase in heat-transfer rates at about $Re_T = 1000$. Simultaneously, a marked decrease in drag coefficient is indicated in Fig. 6. These findings are completely compatible with the mechanism of the phenomenon as outlined in "Principal Considerations"; should transition in the boundary layer occur, increased heat-transfer rates and decrease in drag coefficients should occur simultaneously, and they do.

The significance of the parameter Re_T is notable when the many lines of correlations used by Yuge [8], are plotted in terms of this variable. The data are reduced to a single curve,

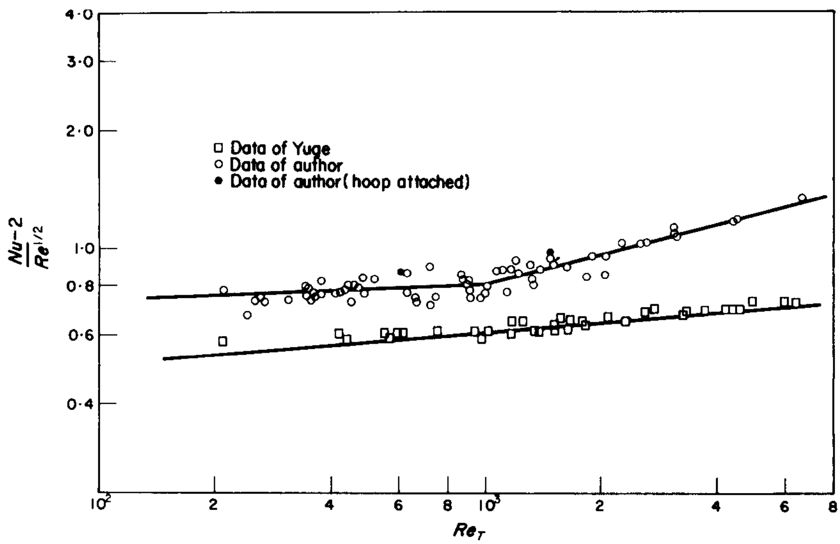

FIG. 5. Relation between Nusselt and turbulent Reynolds numbers.

although unfortunately the heat-transfer rates recorded by Yuge are much lower than those of the author. Since neither set of data produces heat-transfer rates between the two correlations, it is suggested that these two correlations represent upper and lower limits of the rates.

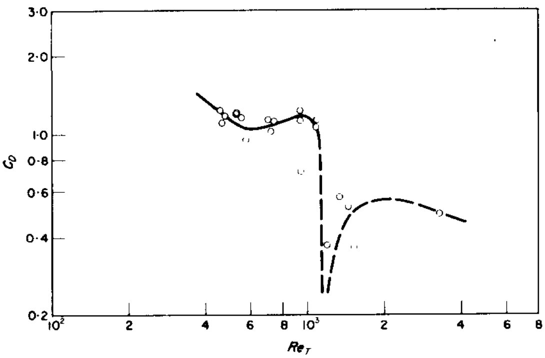

FIG. 6. Relation between drag coefficient and turbulent Reynolds number.

The fact that only Yuge has concluded that free stream turbulence has no effect on the heat-transfer rates indicates that for some reason the wakes of his test pieces have remained the same as that for laminar flow. As a preliminary test of the cause of differences between wakes experienced by the author and those of Yuge, two things were noted:

(i) Yuge operated with a maximum temperature difference between sphere and free stream of about 65 degF, while the author used about 180 degF,

(ii) Yuge reports over 50 per cent increase in heat-transfer rates when an 0·048-in dia. hoop was attached to the forward surface of the sphere.

In order to obtain comparable experimental data, the author, (i) repeated runs with temperature driving forces as low as 10 degF and the heat-transfer rates remained unchanged, (ii) attached an 0·052 in dia. hoop to the forward surface of the sphere, and again noted no significant change in heat-transfer rates. Therefore it must be concluded that Yuge has either not reported or has overlooked some basic parameter which causes the difference.

This argument is further supported by the heat-transfer rates correlated by other workers as shown in Fig. 4. These correlations are more in agreement with the author's data than with Yuge's, although extended somewhat beyond their range. Finally, the Ranz–Marshall correlation was never intended to include turbulent heat-transfer rates and the proximity of this correlation to Yuge's data indicates that the latter has indeed, for some reason, retained a nearly laminar boundary layer.

CONCLUSIONS

(1) This study has succeeded in establishing the turbulent Reynolds number as a single important variable in the phenomenon of turbulent heat transfer.

(2) The introduction of the parameter Re_T is successful in correlating the data of Yuge as well as that of the author.

(3) Upper and lower limits have been proposed for the rate of heat transfer from spheres in a turbulent air stream.

(4) A critical turbulent Reynolds number which causes a marked increase in Nusselt number has been established.

ACKNOWLEDGEMENTS

Financial assistance to one of the authors (W. J. Lavender) from National Research Council of Canada in the form of a research grant is gratefully acknowledged.

REFERENCES

1. O. HINZE, *Turbulence, An Introduction to Its Mechanism and Theory*. McGraw-Hill, New York (1959).
2. H. DRYDEN, G. SCHUBAUER, W. MOCH and H. SKRAMSTAD, Measurements of intensity and scale of wind-tunnel turbulence and their relation to the critical Reynolds number of spheres, NACA TR-581 (1937).
3. L. DAVIS, Measurements of turbulence decay and turbulent spectra behind grids, Report 3–17, Jet Prop. Lab., Pasadena, Calif. (June 1952).
4. L. DAVIS, Measurements of turbulence level behind a set of square-mesh grids and correlation with grid pressure loss, Report 3–22, Jet. Prop. Lab., Pasadena, Calif. (November 1950).
5. E. COMINGS, J. CLAPP J. TAYLOR, Air turbulence and transfer processes—Flow normal to cylinders, *Ind. Engng Chem.* **40**, 1076 (1948).

6. N. Hsu and B. N. Sage, Thermal and material transfer in turbulent gas streams, local transport from spheres, *A.I.Ch.E. Jl* **3**, 405 (1957).
7. B. G. Van der Hegge Zijnen, *Appl. Scient. Res.* **7A**, 205 (1958).
8. T. Yuge, Experiments on heat transfer of spheres—Report 3 (Influence of free stream turbulence at higher Reynolds numbers.) *Rep. Inst. High Sp. Mech., Japan* **11**, 209 (1959–60).
9. C. O. Bennett and J. E. Myers, *Momentum Heat and Mass Transfer*. McGraw-Hill, New York (1962).
10. T. R. Galloway and B. H. Sage, Thermal and material transfer in turbulent gas streams—A method of prediction for spheres, *Int. J. Heat Mass Transfer* **7**, 283 (1964).
11. L. B. Torobin and W. H. Gauvin, Fluid resistance to uniform motion of single spherical particles, *Can. J. Chem. Engng* **37**, 134 (1959).
12. L. B. Torobin and W. H. Gauvin, Fundamental aspects of solids—Gas flow—Part V: The effects of fluid turbulence on the particle drag coefficient, *Can. J. Chem. Engng* **38**, 189 (1960).
13. H. L. Grant and K. T. Nisbet, The inhomogeneity of grid turbulence, *J. Fluid Mech.* **2**, 263 (1957).
14. G. B. Schubauer, W. Spangenberg and P. S. Klebanoff, Aerodynamic characteristics of damping screens, NACA TN-2001, (January 1950).
15. P. Bradshaw, Effect of wind-tunnel screens on nominally two-dimensional boundary layers, *J. Fluid Mech.* **22**, 679 (1965).
16. G. C. Vliet and G. Leppert, Forced convection heat transfer from an isothermal sphere to water, *J. Heat Transfer* **83C**, 63 (1961).
17. W. W. Short, R. A. S. Brown and B. N. Sage, Thermal transfer in turbulent gas streams. Effect of turbulence on local transport from spheres, *J. Appl. Mech.* **27**, 393 (1960).
18. J. Cary, The determination of local forced convection coefficients for spheres, *Trans. Am. Soc. Mech. Engrs* **75**, 483 (1953).
19. G. C. Williams, Sc.D. Thesis in Chem. Engng, M.I.T., p. 265 (1942).
20. W. H. McAdams, *Heat Transmission*. McGraw-Hill, New York (1954).

Résumé—On a étudié dans une souflerie verticale le flux de chaleur à partir d'une sphère de 32 mm de diamètre. Les résultats de transport de chaleur et de traînée indiquent que le produit du nombre de Reynolds par l'intensité de la turbulence, défini sous le nom de nombre de Reynolds turbulent, est un paramètre important, et que l'échelle de la turbulence a moins de sens.

Zusammenfassung—Der Wärmeübergang an einer Kugel von 31,7 mm Durchmesser wurde in einem senkrechten Windkanal untersucht. Die Ergebnisse für Wärmeübergang und Widerstand deuten darauf hin, dass das Produkt aus Reynoldszahl und Turbulenzintensität, das als turbulente Reynoldszahl definiert ist, einen wichtigen Parameter darstellt und, dass der Turbulenzgrad von geringerer Bedeutung ist.

Аннотация—В вертикальной аэродинамической трубе исследовалась интенсивность теплоотдачи от сферы диаметром 1,25 дюйма. Из результатов исследования теплообмена и сопротивления вытекает, что важным параметром является турбулентное число Рейнольдса (определяемое как произведение числа Рейнольдса на степень турбулентности), при этом масштаб турбулентности не имеет существенного значения.